

Nanostructured Interphases and Multiscale Effects in Forming Composite Micro-Rods

*V. M. Harik**

ICASE, MS 132C, NASA Langley Research Center, Hampton VA 23681-2199

ABSTRACT

This article investigates the influence of nanostructured fiber-matrix interphases on the global deformation response and local stress distributions in the composite micro-rods subjected to compressive loads. Finite element modeling of homogeneous and heterogeneous interphases is used to determine parameters that affect the composite response. Linear elastic and nonlinear elastic matrix material models are used in the simulations. Multiscale effects in transverse deformation of micro-rods are examined. The ratio of the matrix and interphase Young's moduli is seen to affect the character of global deformation. A transition from barreling to bollarding type of deformation is seen as this ratio changes. This interphase-controlled change in the deformation mode constitutes a multiscale coupling between the micron-size interphase and the global response of a deforming rod. The radial, hoop, and shear stress distributions in the interphase region are also seen to be highly dependent on the type of interphase present and its submicron property gradients. A special case of theoretical predictions is compared with available data.

* This research was conducted at the Center for Composite Materials, University of Delaware, Newark, DE 19716. Current e-mail: v.m.harik@larc.nasa.gov.

1. INTRODUCTION

Micro-rods made of various materials (e.g., Si, Cu, Au,) are often included in the components of microelectromechanical systems (MEMS). The mechanical (and electric or thermal) properties of micro-rods are essential for MEMS performance [1, 2]. The micro-rod components may be used for micro-cantilevers, micro-resonators, microelectronic devices, and beam-based structures in MEMS (Fig. 1). In the case of micro-cantilevers and micro-resonators, the stiffness of a micro-rod and its thermal conductivity are important material parameters that may significantly affect the vibration frequency and operating conditions of rod-like structures [3]. The vibration frequency is also sensitive to geometric imperfections in the micro-rods. Such requirements considerably limit the choice of ceramic or metallic materials that can be used in these applications.

Composite materials offer an attractive alternative that allows tailoring of the mechanical and thermal properties within a wide range of values of material parameters. Carbon fibers, for example, have very high stiffness and thermal conductivity [4]. An appropriate fiber coating increases durability of the fibers, while a surrounding polymer matrix may protect the coating and serve as an insulator. The net-shape forming of the composite microbeams, which can be made of epoxy matrix and carbon fibers, provides control of geometric imperfections via a one-step forming process by compressive dies. However, the process of net-shape forming can be sensitive to the materials' microstructure [5].

It has been widely recognized that when two material phases are combined during manufacturing of composites, a third phase termed *interphase* is often created [6–8] (Fig. 2). DiAnselmo et al. [9] showed that the interphase may influence the stress and energy distribution in the embedded single-fiber specimens. In the fiber-reinforced epoxy

matrix composites, the interphase thickness may vary from a few nanometers to a few microns, depending on the fiber coating [10]. In a composite, the interphase affects the load transfer between matrix and the reinforcing fibers, the onset of micromechanical damage, and many macroscopic properties such as compression and shear strength, fracture toughness, bulk, and transverse moduli [6, 11–14].

For composite materials with high fiber/volume fractions, interphase regions have considerable total volume and may significantly affect the strength and fracture toughness. Ho and Drzal [15] reviewed earlier studies of interphases and pointed out the importance of local stresses on interphase performance. Interphases having appropriate Young's moduli, Poisson's ratios, and thickness were found to be useful for tailoring bulk properties and reducing stress concentration near interfaces [9, 11]. Interfacial debonding is also influenced by the interface properties [16, 17].

The mechanical properties of a composite micro-rod with a single embedded fiber, its transverse modulus, and its fracture toughness may be also affected by the fiber/matrix interphase, as the studies of DiAnselmo [9] and Harik [18] suggest. Moreover, the secondary processing and press forming of composites or the net-shape forming of micromechanical systems (e.g., MEMS) is dependent on the global and local response under transverse loading. The effect of linear and nonlinear elastic material properties on the transverse deformation of the composite rods has been analyzed by Harik [5] with a finite element model that involved a homogeneous interphase and the barreling-to-bollarding change of deformation modes. Such changes in the global deformation mode may significantly affect the manufacturing of composite micro-rods that require precise geometry. The interphase-to-matrix modulus ratio is the key parameter that controls such a change in the deformation mode. These interphase-controlled changes constitute a multiscale coupling between the micron-size interphase and the global response of a deforming rod.

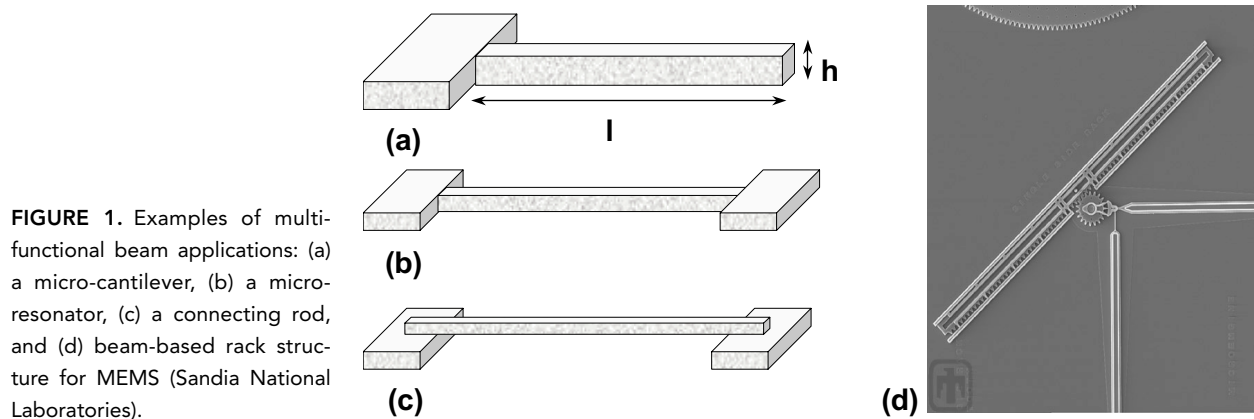


FIGURE 1. Examples of multifunctional beam applications: (a) a micro-cantilever, (b) a micro-resonator, (c) a connecting rod, and (d) beam-based rack structure for MEMS (Sandia National Laboratories).

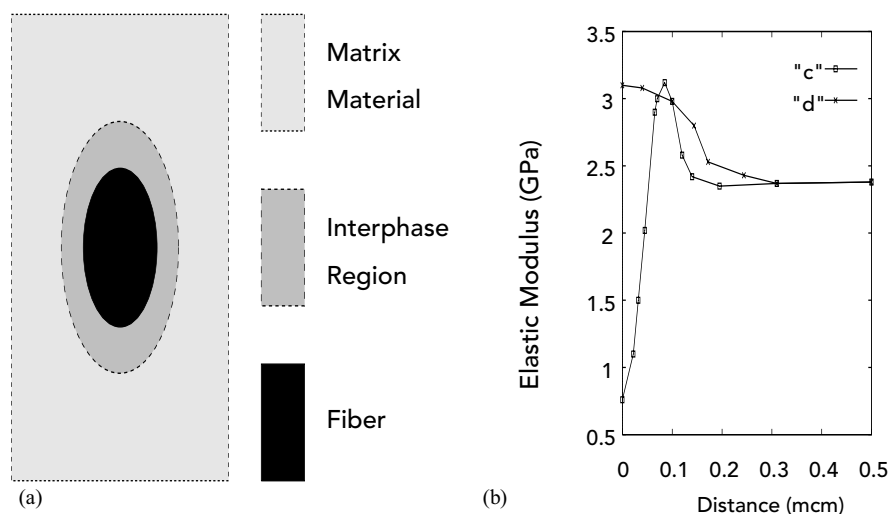


FIGURE 2. Schematic of cross-section of composite micro-rod (a) and variations of interphase modulus (b) based on predictions of Palmese et al. [10]. Interphase "c" is compliant, while case "d" represents a high modulus interphase.

The Young's modulus of the interphasial material depends on the molecular composition of the interphase, the fiber surface coating, and the polymer matrix. Consequently, it may vary with the radial distance from the fiber surface to the surrounding layers of the homogeneous matrix.

Most studies to date have assumed a homogeneous interphase. However, analytical and experimental studies of the interphase region indicate that interphases are in fact heterogeneous [8] (Fig. 2). Figure 2b, which is based on a combination of theoretical and experimental data [10], shows how the Young's modulus may change with the distance from the fiber surface in a fiber-reinforced polymeric matrix composite (PMC). In nanostructured interphases, the property gradients can be significant, on the scale of 100 nm or less. Different variations of interphase stiffness are possible, depending on the composite system, fiber coatings, and processing conditions. Some theoretical and experimental studies have considered heterogeneous interphases, but most assumed a power law variation of the interphase modulus [5, 19, 20].

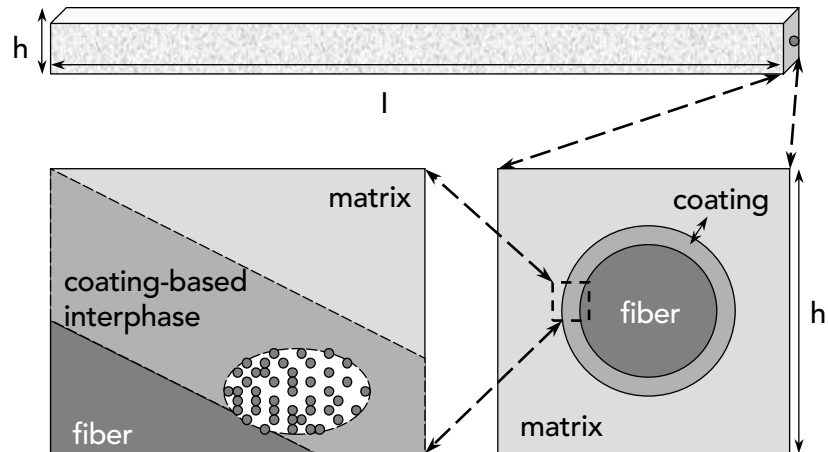
In this article, finite element modeling is employed to carry out a parametric study of homogeneous and heterogeneous nanostructured interphases in the composite micro-rods and their effect on local stresses and the global response of such microsystems. The structural hierarchy of the composite micro-rods and the associated length scales are described in Section 2. The micromechanical finite element model is presented in Section 2.1, along with the model's assumptions. A scaling analysis of the material hierarchy is included in Section 2.2. Numerical results concerning the role of homogeneous and heterogeneous interphases in the process of secondary forming of the composite micro-rods are illustrated in Section 3. The ef-

fect of linear and nonlinear elastic material properties of the polymer matrix on the transverse deformation of micro-rods had been also analyzed. The finite element analysis predicts the barreling-to-bollarding change of deformation modes (Section 3.1), which is an example of multiscale coupling between the micron-size interphase and the global response of the composite rods studied. A special case of theoretical predictions is compared with the available results.

2. FINITE ELEMENT MODELING

The problem of transverse deformation of composite micro-rods involves several length scales: (1) the length of a micro-rod l ; (2) its transverse size h ; (3) the fiber radius R_f and the outer radius of the interphase R_i ; (4) the thickness of the interphase w , or the difference $R_i - R_f$; (5) the scale of local property variations $\Delta l_{\text{elastic}}$; and (6) a characteristic length scale of molecular structures in the interphase $l_{\text{molecular}}$ (Fig. 3). In this analysis, it is assumed that the length of a micro-rod l is such that $l \gg h$, and the plane strain conditions hold. The transverse size of a micro-rod h depends on the fiber radius R_f and its volume fraction at the micrometer length scale. The radius of carbon filaments may vary from about 100 nm to a few microns or tens of microns for traditional carbon fibers [4]. The structure of the composite micro-rods has a kind of macro-micro duality, as its length may be on the order of millimeters while its height has only 40–75 μm (just like a human hair). Later, we will show that a change in the elastic properties of the micron-sized nanostructured interphase may affect the shape of a deforming micro-rod along its entire length.

FIGURE 3. Schematic of structural hierarchy of multifunctional beams that includes several length scales: (1) length of composite micro-rod; (2) transverse dimension of rod or its height; (3) fiber radius; (4) fiber/matrix interphase thickness; (5) characteristic length of interphase property gradients associated with (6) molecular structure involved.



2.1. Micromechanical Model

At the micrometer length scale, a composite micro-rod has a rectangular shape of width l and height h . During a one-step process of net-shape forming, its top and bottom surfaces are subjected to a uniform pressure P , similar to the model of Harik [18]. The lateral boundary, which is allowed to move, is kept traction-free. As a result of symmetry, only one quarter of the micro-rod is modeled (Fig. 4). Along the symmetry lines of the specimen, i.e., $x = 0$ and $y = 0$, zero normal displacements are enforced in the finite element model.

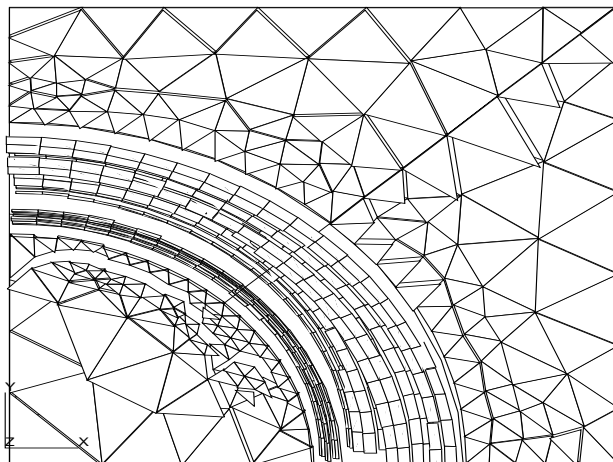


FIGURE 4. Example of mesh of finite elements used in present study. Dimensions are such that $R_f = 1$, $h/2 = 2$, $w_i/R_f = 0.1$.

The carbon fiber and epoxy matrix are assumed to be homogeneous and isotropic materials. The molecular structure of the polymer and its crosslink density are reflected only in the value of its elastic modulus, E_m . That is, [AU: COMMA AFTER "THAT IS" CORRECT?] the smallest material element of the matrix has the bulk material properties. The finite element modeling is based on the quasi-static equilibrium equations for elastic and the Ramberg–Osgood elasto–plastic behavior [18, 21].

The fiber–interphase and interphase–matrix interfaces are considered smooth. The corresponding implicit assumption suggests that the length scale of local property gradients, $\Delta l_{elastic}$ is much smaller than the interphase radius R_i ; $\Delta l_{elastic} \ll R_i$. Both interfaces have perfect adhesion, and plane strain conditions are assumed. The inhomogeneous interphase material is a continuum with uniquely defined material properties—that is, the ratio of a characteristic length scale of molecular structures in the interphase $l_{molecular}$ satisfies an averaging criterion (or homogenization criterion, as suggested by Harik [22])

$$\frac{l_{molecular}}{\Delta l_{elastic}} \ll 1 \quad (1)$$

The thickness of the interphase w_i is larger than the length scale of property variations, $\Delta l_{elastic}$, of course. The smallest dimension of a discrete finite element should be smaller or comparable with such property variations.

An example of a mesh of finite elements used is shown in Fig. 4. It consists of 710 isoparametric triangular and quadrilateral elements with linear interpolation functions. A mesh sensitivity study was conducted. The interphase region has 200 quadrilateral elements, with the element width w_e such that $w_e/R_f = 0.01$, where R_f is the fiber ra-

dus. In the interphase, through-the-thickness variations in material properties are approximated by ten elements, the shape of which reflects the local interface geometry and the lack of circumferential variations. The finite element model developed with the code ABAQUS also allows for some variations in the matrix properties near the interphase, as seen from the mesh structure (Fig. 4).

2.2. Scaling Analysis of Micro-Rod Hierarchy

The multiscale deformation problem described above is characterized by geometric parameters (l , h , R_i , R_f , w_i , $\Delta l_{elastic}$ and $l_{molecular}$) and material parameters (E_m , E_f , E_i , ν_m , ν_f and ν_i). Here, the elastic moduli $E_{()}$ and Poisson's ratios $\nu_{()}$ correspond to the polymer matrix, a carbon fiber, and the interphase, whose structure satisfies the averaging criterion (1). The relative influence of various length scales and material parameters can be evaluated by dimensional and scaling analysis. The dimensional analysis reduces the number of relevant parameters to a minimum set of independent dimensionless parameters.

A scaling analysis of materials hierarchy results in the following five nondimensional ratios:

$$\left\{ \frac{l}{h}, \frac{w_i}{R_f}, \frac{h}{R_f}, \frac{w_i}{\Delta l_{elastic}}, \frac{l_{molecular}}{\Delta l_{elastic}} \right\} \quad (2)$$

which include (1) the length-to-width ratio l/h or the micro-beam aspect ratio; (2) the normalized interphase thickness, w_i/R_f ; (3) the normalized height h/R_f or the fiber volume fraction, $\pi(R_f/h)^2$; (4) the ratio of interphase heterogeneity, $w_i/\Delta l_{elastic}$; and (5) the homogenization ratio, $l_{molecular}/\Delta l_{elastic}$. The aspect ratio l/h is a part of the plane strain condition. The normalized interphase thickness, w_i/R_f , characterizes the interphase volume fraction. The fiber volume fraction, $\pi(R_f/h)^2$, determines the matrix-to-fiber volume ratio. The ratio of interphase heterogeneity, $w_i/\Delta l_{elastic}$ equals unity for homogeneous interphases; it is a large number for highly heterogeneous interphases. The homogenization ratio, $l_{molecular}/\Delta l_{elastic}$ defines an averaging criterion (1) and defines the separation between material microstructure and the nanometer scale molecular structures.

All material parameters can be also reduced to a few nondimensional ratios that have important physical characteristics. Dimensional analysis of these parameters results in the following ratios:

$$\left\{ \frac{E_m}{E_f}, \frac{E_i}{E_m}, \frac{\nu_i}{\nu_f}, \frac{\nu_i}{\nu_m} \right\} \quad (3)$$

The results of this study will demonstrate the key role of the ratio of the interphase-to-matrix moduli, E_i/E_m , in the character of the global deformation of the composite micro-rods. The micron-sized interphase, which is characterized by the normalized interphase thickness, w_i/R_f , may affect the type of deformation mode activated during the compressive forming of the rod having a normalized height, h/R_f , and its final shape along its normalized length, l/h (Section 3.1). Such an interscale interaction illustrates the multiscale coupling present in the forming of the composite micro-rods.

The following numerical results demonstrate how the mechanical properties of the fiber/matrix interphase influence local stresses and the global response of such micro-rods. During the transverse deformation of the micro-rods, the finite element model predicts the barreling-to-bollarding change of global deformation modes.

3. RESULTS AND DISCUSSION

Two different groups of the composite micro-rods are considered: micro-rods with homogeneous interphases and those with inhomogeneous interphases. In both cases, linear and nonlinear material properties and deformation are analyzed. In all cases the fiber and matrix were considered homogeneous, and all constituents were assumed to be isotropic.

3.1. Homogeneous Micron-Size Interphases

In this section, two representative cases of homogeneous interphases are described. One has $E_i = 375.0$ MPa and $\nu_i = 0.4$; the other has $E_i = 37.5$ MPa and $\nu_i = 0.4$. The second, more compliant, case would correspond to an interphase in a polymer material near its glass transition temperature. Such a decrease in the interphase Young's modulus may be caused by various heat effects or processing conditions [10]. In both cases the size of the interphase is kept at $w_i/R_f = 0.1$. For the linear elastic case, the Young's moduli and the Poisson's ratios used are $E_f = 241$ GPa, $\nu_f = 0.25$ for the fiber and $E_m = 2.5$ GPa, $\nu_m = 0.363$ for the matrix. This system is meant to simulate a micro-rod made of a graphite/epoxy composite rod. In the finite element model, the micro-rod dimensions were such that $R_f = 1$, $h = 4$, and $l = 20$.

For homogeneous interphases with $E_i = 375.0$ MPa and $E_i = 37.5$ MPa, the displacement contour plots are similar to the results of Harik [18]. The loads are small enough so that a linear elastic response of the matrix and interphase is assured. This study shows that the values of stresses in the homogeneous interphase with $E_i = 375.0$

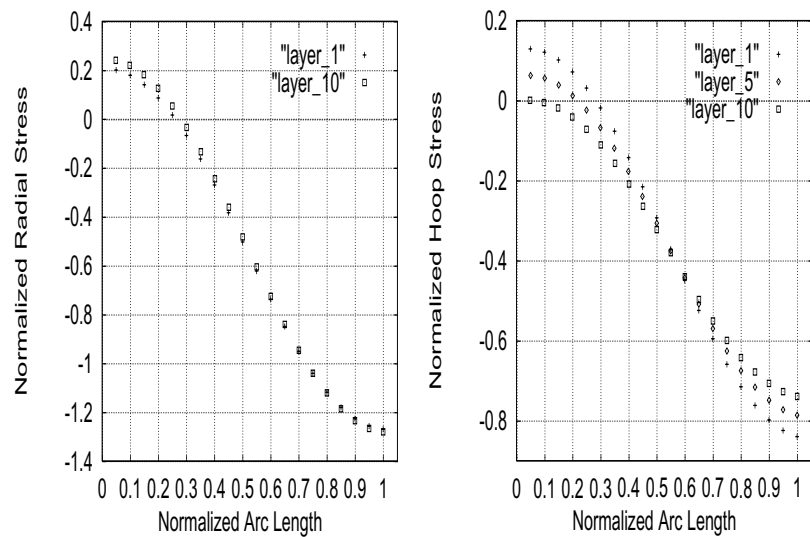


FIGURE 5. Distributions of radial and hoop stresses normalized by transverse load in layers of elastic interphase region such that $E_i = 375.0$ MPa, $\nu_i = 0.4$, $w_i/R_f = 0.1$.

MPa (Fig. 5) are favorable for the nucleation of an interfacial crack. The radial and hoop stresses are predicted along the circumferential arc in counterclockwise direction starting from the horizontal axis at $y = 0$. Near this axis, the radial stress has positive values, while the hoop stress changes its sign, which that may result in radial and/or circumferential microcracks. In the absence of any property gradients, the radial stress does not vary across the interphase (Fig. 5a). Naturally, it becomes highly compressive near the top of the fiber (i.e., 90° arc angle). The hoop stresses vary more across the interphase because of the nonuniform hoop strains induced by the local shear. Hence the extra layer of data points in Fig. 5b.

Nucleation of an interfacial crack is possible, especially because the stresses are not reduced for the more compliant interphase, $E_i = 37.5$ MPa, as one would expect in a parametric study. However, this paradox is explained by the difference in the global response of the composite rods, which depends on the modulus of the interphase. For a high value of E_i , the composite exhibits bollarding—i.e., the dominant expansion at the top and bottom of the specimen (Fig. 6a). However, when E_i is decreased, the global mode of deformation switches to barreling, which leads to higher strains along the center line ($y = 0$, Fig. 6b). A parametric study of the variations in the ratio E_i/E_m show that this transition occurs at about 0.06 (i.e., $E_i = 150$ MPa) for the parameters used. This result implies that there is an optimal interphase-to-fiber-modulus ratio, and therefore an operating temperature, at which the specimen surface would not deform, thus aiding in the net-shape forming.

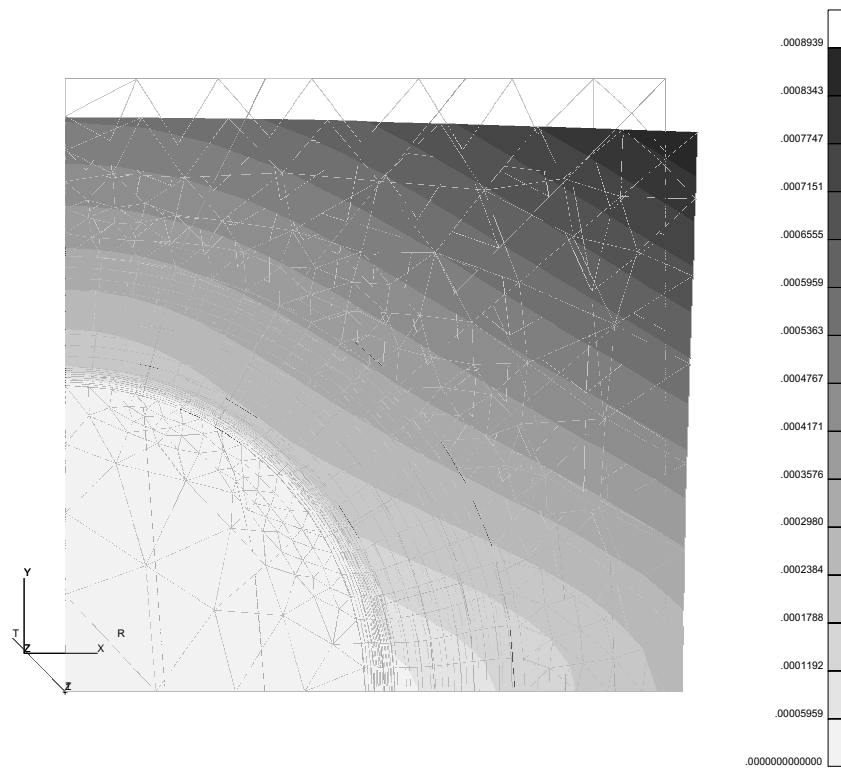
Numerical simulations were also carried out with a nonlinear Ramberg–Osgood interphase having the yield stress

of 35 MPa, yield offset of 0.07, and hardening exponent of 5.5 [5]. For the magnitude of total displacements (Fig. 6), the results produced were similar to the linear elastic response of the composite [18]. The governing parameter that determines the deformation mode is still the ratio of elastic moduli, E_i/E_m , as for the linear elastic case. The critical value, 0.06, of this ratio was not changed by the variations of nonlinear elastic–plastic parameters. However, bollarding was seen to develop for the uniform nodal forces applied to the second-order elements, which corresponds to periodically varying stresses, even though E_i was 37.5 MPa.

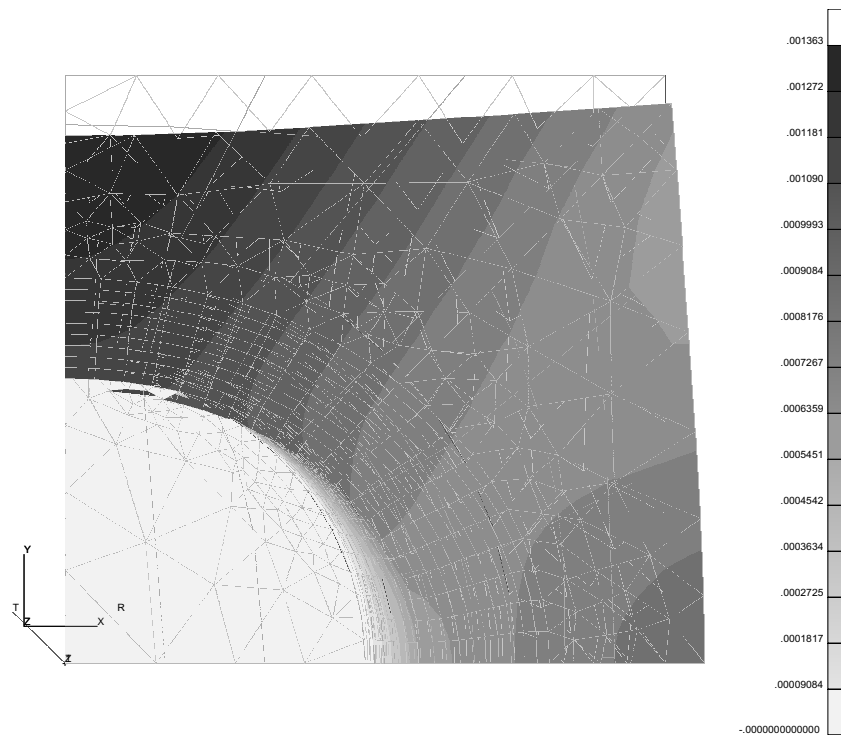
The size of geometric imperfections (e.g., an indent in the middle of the top and the bottom surfaces of the barreling micro-rod, Fig. 6b) primarily depends on the normalized thickness, w_i/R_f , of compliant interphases and the matrix Poisson's strains characterized by the corresponding Poisson's ratio. In the case of asperities on both sides of the bollarding micro-rod near its top and bottom, Fig. 6a, the normalized height h/R_f is important, as opposed to the thickness of hard interphases. An interphase with the Young's modulus close to that of the matrix simply extends an effective volume of the polymer matrix, while the much harder interphases contribute to an effective fiber radius and the fiber volume fraction.

3.2. Heterogeneous Nanostructured Interphases

Experimental and theoretical results have shown that the interphase created in fiber-reinforced PMCs is, in fact, heterogeneous. Two typical property variations of the interphase are shown in Fig. 2b (after Palmese et al. [10]).



(a)



(b)

FIGURE 6. Original wire-frames of finite elements and contour plots of magnitude of total displacement for (a) bollarding deformation mode for $E_i = 375.0$ MPa; (b) barreling deformation mode for $E_i = 37.5$ MPa.

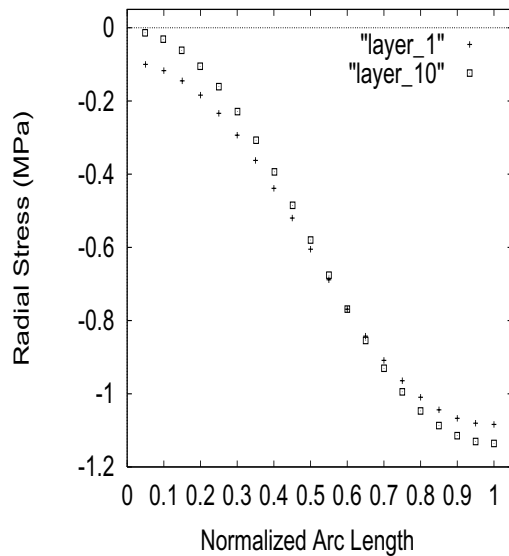


FIGURE 7. Distribution of radial stress in (a) heterogeneous “d” interphase with Young’s modulus variations between 3.2 GPa and 2.5 GPa (i.e., matrix modulus).

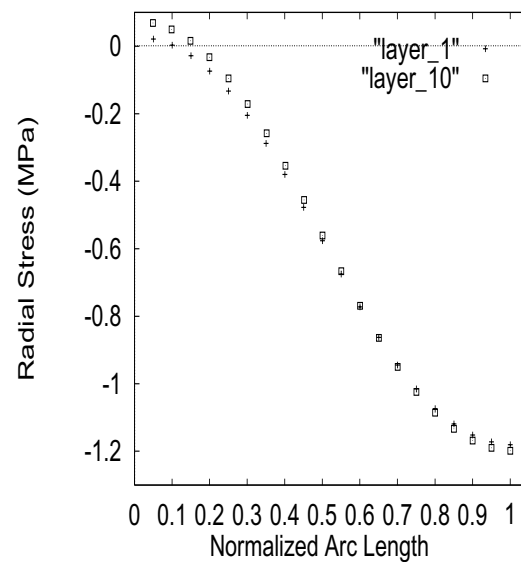


FIGURE 8. Distribution of radial stress along heterogeneous compliant “c” interphase with Young’s modulus variations between 760 MPa and 2.5 GPa (i.e., matrix modulus).

Although a homogeneous assumption may in some cases be a reasonable approximation to an interphase with low property gradients—e.g., case (d) in Fig. 2b, while case (c) involves large variations in modulus. In this part of the study, the effect of a heterogeneous interphase on the local stress distribution and global deformation of the composite micro-rods is investigated.

Figures 7 and 8 show the variation of radial stresses with the arc length along the fiber starting from the point ($x = R_f, y = 0$) at several radial stations in the heterogeneous interphases. Figure 7 corresponds to the model “d” of a high modulus interphase and Fig. 8 to the model “c” of a compliant interphase. Interphase heterogeneity led to values of the radial stress that are considerably lower than those found in any of the homogeneous interphases. In particular, the radial stress values in the compliant interphase with a large variation of Young’s modulus, Fig. 8, are much lower than those in the homogeneous interphases with $E_i = 375.0$ MPa and $E_i = 37.5$ MPa. The hoop stress also drops significantly away from the fiber surface.

The distributions of the shear stress in the interphase region for the interphase models “c” and “d” indicate that the maximum shear stresses in both cases are reached at the interphase–fiber interface (at 45° from the horizontal line of symmetry). Unlike the radial and hoop stresses, the shear stress values are higher than those for the two homogeneous interphases. Such redistribution of shear stresses at the fiber–interphase interface suggests a higher probability of shear-induced localized failure. The interfacial

shear strength of the composites with the larger variation of the Young’s modulus (case “c”) seems to be lower than that of the composites with the stiffer inhomogeneous interphases (case “d”).

Note that the barreling–bollarding change in the global deformation mode does not occur for the considered cases of heterogeneous interphases, because the interphase Young’s modulus, E_i , has not reached low enough values. That is, the ratio E_i/E_m is much higher than its transition value of about 0.06 (i.e., $E_i = 150$ MPa) for the parameters used.

4. CONCLUSIONS

This study has examined the influence of homogeneous and heterogeneous fiber–matrix interphases on global deformation modes and local stress distributions in composite micro-rods when they are subjected to transverse compressive loads, as in the forming processes. The finite element modeling of the composite micro-rods with homogeneous interphases showed that the ratio of the matrix and interphase Young’s moduli affects not only the local stress distribution, but also the global deformation response. A transition from the barreling to the bollarding type of deformation has been observed. The critical material parameters that affect the micro-rod response have been determined. The ratio of the matrix-to-interphase Young’s moduli has been shown to affect the character of global deformation. This interphase-controlled change in the deformation mode

constitutes a multiscale coupling between the micron-size interphase and the global response of a deforming micro-rod. Simulations of two types of heterogeneous interphases showed that the radial, hoop, and shear stress distributions in the interphase region are also highly dependent on the type of interphase heterogeneity present. Linear and nonlinear elastic matrix material models have been used in the analysis. The length-scale issues in the transverse deformation of the micro-rods have been examined, along with the material structural hierarchy. A special case of theoretical predictions is compared with the available data.

REFERENCES

1. Lyshevski, S. E. *Nano- and Microelectromechanical Systems*, CRC Press, New York, 2001.
2. Varadan, V. K. and Zoelzer, U. *RF MEMS & Their Applications*, Wiley, New York, 2002.
3. Timoshenko, S. *Vibration Problems in Engineering*, 3rd edition. Van Nostrand, New York, 1955.
4. Chang, D. D. L. Comparison of submicron-diameter carbon filaments and conventional carbon fibers as fillers in composite materials. *Carbon* 39:1119–1125, 2001.
5. Harik, V. M. Experimental and theoretical studies of interfacial effects in multiphase media. PhD thesis, University of Delaware, Newark, DE, 1997.
6. Drzal, L. T. The interphase in epoxy composites. *Adv. Polym. Sci.* 75:1–32, 1986.
7. Hughes, J. D. H. The carbon fiber/epoxy interface—a review. *Composites Sci. Tech.* 41:13–45, 1991.
8. Palmese, G. R. and McCullough, R. L. Effect of epoxy amine stoichiometry on cured resin material properties. *J. Appl. Polym. Sci.* 46(10):1863–1873, 1992.
9. DiAnselmo, A., Accorsi, M. L., and DiBenedetto, A. T. The effect of an interphase on the stress and energy distribution in the embedded single fiber test. *Composites Sci. Tech.* 44:215–225, 1992.
10. Palmese, G. R., McCullough, R. L., and Sottos, N. R. Relationship between interphase composition, material properties and residual thermal stresses in composite materials. *J. Adhesion* 52(1–4):101–113, 1995.
11. Tsai, H. C., Arocho, A. M., and Gause, L. W. Prediction of fiber–matrix interphase properties and their influence on interface stress, displacement and fracture toughness of composite material. *Mater. Sci. Eng.* A126:295–304, 1990.
12. Sottos, N. R., Li, L., and Agrawal, G. The effects of interphase properties on interfacial shear strength in polymer matrix composites. *J. Adhesion* 45:105–124, 1994.
13. Lutz, M. P. and Zimmerman, R. W. Effect of the interphase zone on the bulk modulus of a particulate composite. *J. Appl. Mech.* 63:855–861, 1996.
14. Wacker, G., Bledzki, A. K., and Chate, A. Effect of interphase on the transverse Young's modulus of glass/epoxy composites. *Composites Part A*, 29A:619–626, 1998.
15. Ho, H. and Drzal, L. T. Evaluation of interfacial mechanical properties of fiber reinforced composites using the microindentation method. *Composites Part A*, 27A: 961–971, 1996.
16. Haddadi, H. and Teodosiu, C. 3D analysis of the effect of interfacial debonding on the plastic behavior of two-phase composites. *Comp. Mater. Sci.* 16:315–322, 1999.
17. Harik, V. M. and Cairncross, R. A. Evolution of interfacial voids around a cylindrical inclusion. *J. Appl. Mech.* 66(2): 310–314, 1999.
18. Harik, V. M. Response of composites under compressive loads: finite element modeling of interphase effects. *J. Mech. Behav. Mater.* 8(1):29–39, 1997.
19. Jasiuk, I. and Kouider, M. W. The effect of an inhomogeneous interphase on the elastic constants of transversely isotropic composites. *Mech. Mater.* 15:53–63, 1993.
20. Low, B. Y., Gardner, S. D., Pittman, C. U. J., and Hackett, R. M. A micromechanical characterization of graphite/epoxy composites containing a heterogeneous interphase region. *Composites Sci. Tech.* 52(4):589–606, 1995.
21. Bathe, K.-J. *Finite Element Procedures in Engineering Analysis*. Prentice Hall, Englewood Cliffs, NJ, 1982.
22. Harik, V. M. Mechanics of carbon nanotubes: applicability of the continuum-beam models, *Computat. Mater. Sci.* 24: 328–342, 2002.

ACKNOWLEDGMENTS

This research was supported by the Center for Composite Materials (CCM) and the Department of Mechanical Engineering of the University of Delaware. Useful discussions with Professors J. Lambros (University of Delaware/University of Illinois) and G. R. Palmese (University of Delaware/Drexel University) and Drs. T. A. Bogetti and X. Huang (CCM/US Army Research Lab) are gratefully acknowledged. The final analysis was supported in part by the NASA Langley Research Center.